

# Tunable external-cavity diode laser based on integrated waveguide structures

Kevin S. Repasky  
Jennifer D. Williams  
John L. Carlsten  
Montana State University  
Spectrum Lab and Department of  
Physics  
Bozeman, Montana 59717

Elizabeth J. Noonan  
Gregg W. Switzer  
AdvR  
910 Technology Boulevard, Suite K  
Bozeman, Montana 59718

**Abstract.** Ion diffusion of rubidium (Rb) in potassium titanyl phosphate (KTP) creates areas of high Rb concentration. The areas of high Rb concentration have an index of refraction of  $n_{\text{Rb}} = 1.846$  as compared to the index of refraction for the KTP of  $n_K = 1.842$ . The small change in the index of refraction is enough to create waveguide structures and integrated optics such as Bragg gratings in the KTP substrate. A tunable external-cavity diode laser is constructed using waveguide structures and integrated optics created by this ion diffusion. The resulting Bragg grating is used to provide optical feedback to control the operating wavelength of an external-cavity laser. Tuning is accomplished using the electro-optic properties of KTP to control the effective period of the Bragg grating. A tuning response of  $R = 19.5 \text{ MHz/V}$  was measured. © 2003 Society of Photo-Optical Instrumentation Engineers. [DOI: 10.1117/1.1590319]

Subject terms: external-cavity diode lasers; waveguide structures; electro-optic devices; tunable lasers.

Paper 020474 received Oct. 28, 2002; revised manuscript received Jan. 24, 2003; accepted for publication Feb. 10, 2003.

## 1 Introduction

Diode lasers work in the near-IR (800- to 1600-nm) spectral region, where many important atmospheric molecules,<sup>1,2</sup> chemicals,<sup>3</sup> and pollutants<sup>1,2</sup> will absorb light. Because of their spectral coverage, diode lasers are finding applications in areas such as atomic physics,<sup>4</sup> remote sensing,<sup>2,3,5</sup> and chemical detection systems.<sup>3,6</sup> Diode lasers have many positive attributes including efficiency at converting electrical power to optical power and compact packaging that make them ideal candidates as sources for laser detection. However, diode lasers do not always operate in a single longitudinal mode or at the appropriate wavelength of interest.

External cavity diode lasers<sup>7-10</sup> have been built enabling tunable single-mode laser operation. These lasers rely on optical feedback to control the wavelength of the laser diode. Typically, a diffraction grating is used to spatially separate the spectral components of the diode laser output. One spectral component is fed back to the diode laser, forcing it to operate at the wavelength of the optical feedback. In the case of a Littrow configuration,<sup>7,8</sup> the first-order reflection from the diffraction grating is used to provide the optical feedback. For the Littman-Metcalf configuration,<sup>9,10</sup> the first-order reflection from the diffraction grating is incident on a retroreflector, which directs the optical feedback back to laser diode via a second reflection from the diffraction grating. Tuning of the external-cavity diode laser is accomplished by mechanically moving either the diffraction grating or the retroreflector such that a different spectral component is fed back to the laser diode.

Ion diffusion of rubidium (Rb) in a potassium titanyl phosphate (KTP) crystal<sup>11</sup> creates areas of high index of refraction that coincide with the areas of high Rb concentration. The diffusion of Rb increases the average index of

refraction of the waveguide by approximately 0.1% compared to the index of refraction for undoped KTP. This increase is enough to create integrated optical components such as optical waveguides and Bragg gratings. KTP also has electro-optic properties that enable electronic control of the index of refraction as a function of applied voltage across the KTP substrate.

The integrated optics that can be written into KTP via ion exchange can be used to create a tunable external-cavity diode laser. A Bragg grating can provide the spectrally filtered optical feedback required to control the operating wavelength of the laser. Tuning the laser can be accomplished electronically by utilizing the electro-optic properties of the KTP material. A control voltage applied across the integrated Bragg grating will change the effective Bragg period due to the change in the net index of refraction caused by the electro-optic effect. This changes the spectral component of light fed back to the diode laser, thus forcing the diode laser to operate at the new wavelength. One advantage of building a tunable external-cavity diode laser based on integrated optics is that the integrated construction of the laser eliminates the need for mechanically moving parts. The laser is more stable against low-frequency noise due to mechanical vibrations. A second advantage of the waveguide-based external cavity diode laser is the potential compact size, on the order of  $10 \times 10 \times 10 \text{ mm}$ .

A tunable external cavity based on waveguide structures is described in this paper. Section 2 contains the details of the design and construction of the integrated optics. Section 3 discusses the electro-optic tuning of the laser. The performance of the waveguide-based external-cavity diode laser is presented in Sec. 4. Finally, Sec. 5 provides some brief concluding remarks.

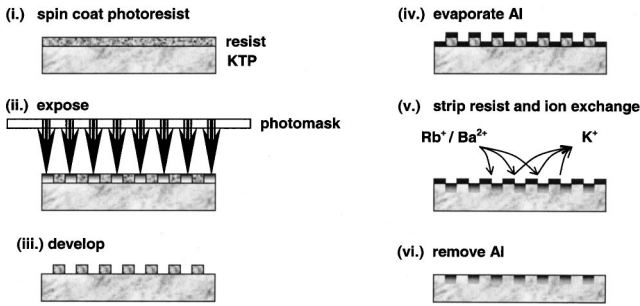


**Fig. 1** Six-step process used to create the waveguide structure in the KTP substrate. The first four steps of this process were done at the Cornell Nanofabrication Facility in Ithaca, New York.

## 2 Waveguide Design and Construction

Waveguide structures can be created in KTP using the process shown in Fig. 1. First, a photoresist is deposited on the top of a KTP substrate. The photoresist is exposed through a photomask by an arc lamp. The developing process removes the photoresist material that was exposed to the arc lamp. Next, a layer of aluminum is evaporated onto the remaining photoresist material and exposed KTP. These first four steps were performed at the Cornell Nanofabrication Facility in Ithaca, New York. The remaining photoresist material is removed with acetone, leaving aluminum covering the KTP material where the KTP was exposed to the arc lamp through the photomask. The KTP material is next placed in a  $\text{Rb}^+/\text{Ba}^{2+}$  bath. The rubidium diffuses into the KTP substrate through the openings in the aluminum pattern and replaces the potassium.<sup>11</sup> The diffusion along the  $z$  axis is  $\sim 10^4$  greater than along the  $x$  or  $y$  direction, creating well-defined boundaries within the waveguide. The ion-exchange rate is well known so that the depth of the waveguide can be controlled to within  $\pm 1 \mu\text{m}$ . The final step involved in the creation of the waveguide structure is the removal of the aluminum. This is accomplished by dipping the KTP substrate into a solution of potassium hydroxide (KOH).

The waveguide structure is shown in Fig. 2 and contains two distinct regions: a channel section and a Bragg section. The channel section is made up of a series of rhomboids, which were chosen to eliminate back reflection to the diode

laser. The Bragg region is made up of a series of rectangles, which were chosen to generate a back reflection to the diode laser. The shaded areas for both regions have a higher index of refraction, relative to the host KTP, due to the ion exchange process.

The properties of the waveguide structure are governed by the difference in the index of refraction between the areas of high rubidium concentrations. These properties are first estimated mathematically then verified experimentally. The effective index of refraction  $n_{\text{eff}}$  of the waveguide depends on  $n_{\text{KTP}}$ ,  $n_{\text{Rb}}$ ; and the modal index of refraction  $n_{\text{modal}}$ , which depends on the geometry of the waveguide. The  $n_{\text{KTP}}$  is determined by using the Sellmeier equations ( $n_{\text{KTP}} = 1.844 \pm 0.001$ ). The effective index of  $n_{\text{Rb}}$  and  $n_{\text{modal}}$  is measured experimentally using the following method. A broadband light source such as an LED illuminates a KTP waveguide with a similar geometry as that being designed. The spectral output is measured on an optical spectrum analyzer (OSA) and the center wavelength  $\lambda$  of the Bragg reflection is identified to within  $\pm 0.1 \text{ nm}$  (the resolution of the OSA.) The effective index can then be determined from the Bragg condition  $m\lambda = 2n_{\text{eff}}\Lambda$ , where  $m$  is an integer (the Bragg order),  $\Lambda$  is the Bragg spacing, and  $n_{\text{eff}} = D_o n_{\text{KTP}} + D_i(n_{\text{Rb}}) + n_{\text{modal}}$ , where  $D_i/D_o$  is the duty cycle, the fraction of the total Bragg spacing. The duty cycle for both regions is 50/50 so they have the same waveguiding properties. Another way of estimating the index of refraction is by modeling the actual waveguide geometry on a mode solver to include modal index. This was not available.

The resulting waveguide is single spatial mode with a numerical aperture of  $\sim 0.2$  and  $M^2 \leq 1.2$ . Fresnel reflection of the air/waveguide interface is  $\sim 9\%$  at 800 nm. Propagation loss is estimated to be 1.0 dB/cm for typical segmented channel waveguides,<sup>12</sup> corresponding to 21% loss for our waveguide. The coupling efficiency depends on the input beam. Asymmetric beam profile and astigmatism associated with a  $1 \times 3\text{-}\mu\text{m}$  aperture of the diode laser leads to a coupling efficiency of 31% excluding Fresnel losses at the front and back facets and propagation loss of the waveguide.

A schematic for a tunable external cavity diode laser based on an integrated waveguide structure is shown in Fig.

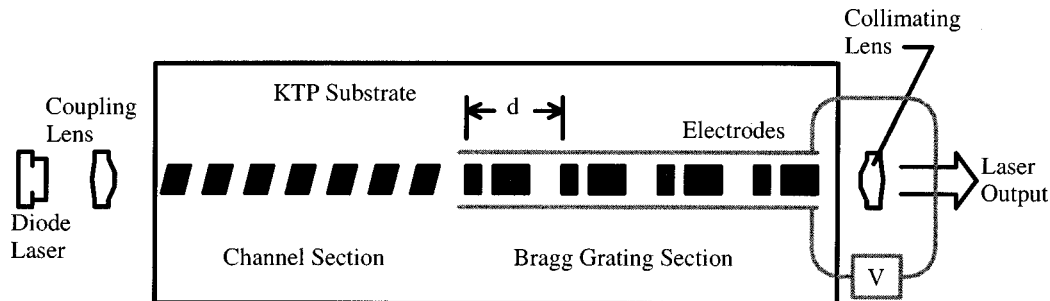


**Fig. 2** Schematic of the waveguide-based tunable external-cavity diode laser. The diode laser is coupled into the waveguide structure written into the KTP substrate via ion exchange. The waveguide structure is made up of a channel section that confines the beam and a Bragg grating section that provides optical feedback. The laser is tuned by exploiting the electro-optic properties of the KTP crystal.

2. Light from a diode laser is coupled into a waveguide that has been created in KTP via ion exchange. The waveguide contains a channel section that confines the light and a Bragg grating that provides the optical feedback used to control the operating wavelength of the external cavity laser. A collimating lens collects light leaving the waveguide.

The waveguide design is governed by the change in the index of refraction when the rubidium replaces the potassium. A single spatial mode will propagate in the waveguide when the normalized cutoff frequency  $V$  meets the condition<sup>13</sup>

$$V = \frac{\pi a}{\lambda} (n_{\text{WG}}^2 - n_{\text{K}}^2)^{1/2} < 2.406, \quad (1)$$

where  $a$  is the width of the waveguide structure. A waveguide based on ion-exchanged KTP will support a single spatial mode at 800 nm when  $a < 3.6 \mu\text{m}$ .

The Bragg grating was numerically modeled in the following manner. The reflection at the interface of two different indices of refraction  $R$  is given by

$$R = \left( \frac{n_{\text{Rb}} - n_{\text{K}}}{n_{\text{Rb}} + n_{\text{K}}} \right)^2, \quad (2)$$

and the transmission is given by  $T = 1 - R$ . An electric field at a particular wavelength is incident on the Bragg grating. The electric field is propagated through a Bragg period, keeping track of the phase. The reflection and transmission is calculated at each interface of high and low indices of refraction. These beams are again propagated through another Bragg period, keeping track of the phase. This process is repeated until the beam has gone through the entire set of designed periods in such a way that the total reflection and transmission of the electric field from the entire Bragg grating is determined. We assume that the electric field is a vertically polarized plane wave, the change in the index from that of KTP is known beforehand, and the Bragg period is perfectly regular. No overlap integral was used in this calculation.

A simple Bragg grating is made up of a Bragg element with one segment of high index of refraction and one segment of low index of refraction. The Bragg elements are repeated with a specific periodicity to create a Bragg grating. A simple Bragg grating with a duty cycle of 50/50 contains segments of high and low indices of refraction of equal length. Numerical calculations were performed for a simple Bragg grating with a Bragg period of  $8.8 \mu\text{m}$ . A plot of the reflectivity as a function of wavelength is shown in Fig. 3. A peak reflectivity of 30% is expected at the wavelength of 793 nm. If the length of the high index of refraction section is increased by 88 nm so that the duty cycle is 49/51, the reflection from the simple Bragg grating drops below 5%.

A super Bragg grating is shown in Fig. 2. A Bragg period consists of two regions of low index of refraction and two regions of high index of refraction. A duty cycle of 50/50 means there is an equal area of high and low indices of refraction. A plot of the reflectivity as a function of wavelength is shown in Fig. 4 for the super Bragg grating. The solid line represents calculations for the 50/50 duty

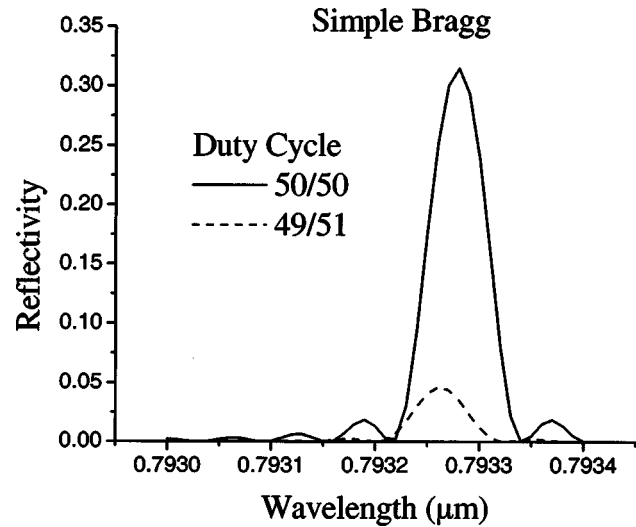


**Fig. 3** Theoretical model of the reflectivity as a function of wavelength for a simple Bragg grating. The solid line is the numerical modeling results for a simple Bragg grating with a duty cycle of 50/50, while the dashed line represents the results of the numerical modeling for a duty cycle of 49/51. The change in the duty cycle drops the maximum reflectivity from 32 to 5%.

cycle, while the dashed line represents the calculations for the 49/51 duty cycle. The maximum reflectivity for the 49/51 duty cycle has a peak value of 18%. During the course of creating the mask and photolithographically adhering the mask onto the KTP wafer, the duty cycle can change due to the tolerances associated with these processes. The reflectivity of the super Bragg grating is less susceptible to the change in duty cycle due to the manufacturing process and is thus used.

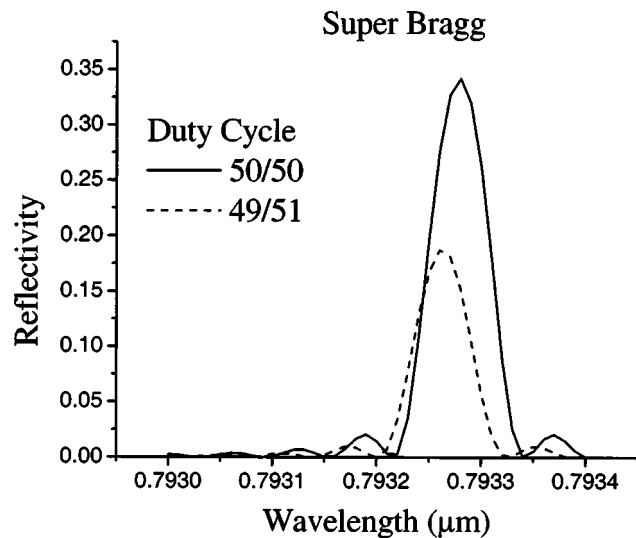


**Fig. 4** Theoretical model of the reflectivity as a function of wavelength for a super Bragg grating. The solid line is the numerical modeling results for a super Bragg grating with a duty cycle of 50/50, while the dashed line represents the results of the numerical modeling for a duty cycle of 49/51. The change in the duty cycle drops the maximum reflectivity from 34 to 20%. The super Bragg grating is less susceptible to the tolerances associated with generation of the waveguide structures.

**Table 1** The design parameters for the 10 different waveguides created in the KTP substrate via ion exchange.

Guide No.	Peak Wavelength (nm)	Peak Reflectivity (%)	Bragg Period ( $\mu\text{m}$ )	Number of Bragg Periods	Reflection Linewidth (GHz)
1	793.36	89	9.44	424	29
2	792.96	72	14.16	283	24
3	793.1	85	10.30	390	29
4	793.28	59	8.80	455	24
5	793.34	52	18.46	217	24
6	793.40	74	12.88	311	24
7	793.48	79	13.74	292	24
8	793.54	40	21.90	183	24
9	1548.70	74	13.61	294	26
10	1550.18	87	10.24	391	31

A total of 30 waveguides are created in a 10-mm-long by 3-mm-wide by 1-mm-thick KTP substrate. Ten different waveguide structures are repeated in three clusters. The design parameters for each of the 10 waveguides are listed in Table 1.

### 3 Laser Tuning

KTP is an electro-optic crystal and thus the index of refraction is a function of the applied voltage. This property of the KTP crystal can be used to tune the laser in one of the two following ways, depending on whether the voltage is applied across the channel section or the Bragg grating section.

An optical cavity is formed between the back facet of the laser diode and the front of the Bragg grating. An integer number of half wavelengths must fit within this cavity for optical power to circulate. Applying a voltage across the channel section of the waveguide enables the cavity length to change due to the change in the index of refraction resulting from the electro-optic properties of the KTP substrate. If the cavity length is changed while the number of half wavelengths remains constant, then the wavelength must change to maintain the resonant condition for the cavity. The change in frequency  $\Delta\nu_c$  is related to the applied voltage  $V$  by<sup>14</sup>

$$\Delta\nu_c = \frac{\nu n^3 l r}{2l_{\text{cav}} d} V, \quad (3)$$

where  $\nu$  is the laser center frequency,  $n$  is the index of refraction of the channel section,  $l$  is the length of the channel section,  $r$  is the electro-optic coefficient and  $r = 36 \text{ pm/V}$  for KTP,  $l_{\text{cav}}$  is the external cavity length, and  $d$  is electrode spacing. For  $l = 1 \text{ cm}$ ,  $l_{\text{cav}} = 5 \text{ cm}$ ,  $d = 2 \text{ mm}$ , and  $\lambda = 800 \text{ nm}$ , the tuning response is  $R = \Delta\nu/V = 0.43 \text{ MHz/V}$ .

Light reflected by the Bragg grating provides optical feedback to the laser diode and forces the laser to operate at a particular wavelength. Applying a voltage across the Bragg grating section changes the index of refraction and thus changes the wavelength of light reflected from the grating. The laser will operate at this new wavelength be-

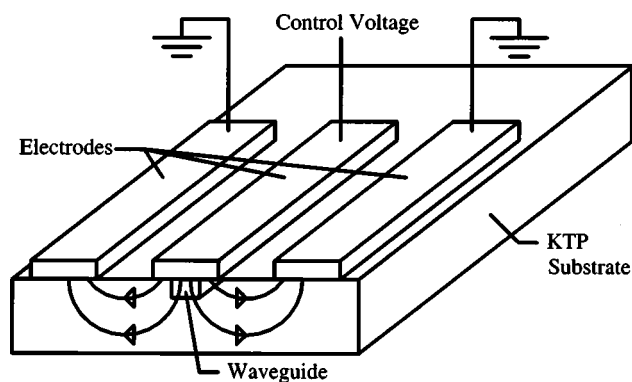


**Fig. 5** Schematic of the electrodes that supply the control voltage for electro-optic tuning of the laser. The electrodes are deposited onto a glass substrate and aligned using an optical microscope. The glass substrate is glued to the KTP substrate with UV cure epoxy.

cause of the optical feedback. The frequency tuning can be calculated by starting with the Bragg condition  $M\lambda = n\Lambda$ , where  $M$  is an integer,  $n$  is the index of refraction, and  $\Lambda$  is the Bragg period. Using the relationship<sup>15</sup>  $\Delta n/\Delta V = -(n^3 r)/(2d)$ , the change in frequency as a function of applied voltage can be written

$$\Delta\nu_g = \frac{\nu^2 \Lambda n^3 r}{2cMd} V, \quad (4)$$

where  $c$  is the speed of light. For  $\Lambda = 8.8 \mu\text{m}$ ,  $M = 11$ ,  $\lambda = 800 \text{ nm}$ , and  $d = 2 \text{ mm}$ , the tuning response for KTP is  $R = \Delta\nu/V = 21.2 \text{ MHz/V}$

A schematic of the electrodes used to control the Bragg grating spacing via the electrooptic effect is shown in Fig. 5. The electrodes are made by depositing gold onto a glass substrate. The ground planes are  $62 \mu\text{m}$  wide while the electrodes used to apply the control voltage are  $20 \mu\text{m}$  wide. The spacing between the electrodes is  $6 \mu\text{m}$ . A total of eight ground planes and eight control voltage electrodes are deposited onto the glass substrate. The electrodes are aligned using a microscope so that the waveguide is under the edge of a control voltage electrode. The glass substrate and KTP substrate are then joined using UV cure epoxy.

### 4 Laser Performance

A picture of the waveguide test assembly is shown in Fig. 6. A laser diode with a center wavelength of  $796 \text{ nm}$  is collimated using a lens with a focal length of  $f = 3.10 \text{ mm}$  and a numerical aperture of  $\text{NA} = 0.68$  (Thor Labs C330TM-B). Light is next incident on a second lens with a focal length of  $f = 4.5 \text{ mm}$  and a numerical aperture of  $\text{NA} = 0.55$  (Thor Labs CM230TM-B). The second lens is used to couple the diode laser into the waveguide. A third lens is used to collimate the light exiting the waveguide structure.

The KTP substrate and electrode assembly is mounted so that both waveguide selection and alignment can be accomplished. Waveguide selection is achieved using a translation stage (New Focus 9065-X) that moves the KTP substrate perpendicular to the beam. Alignment of the

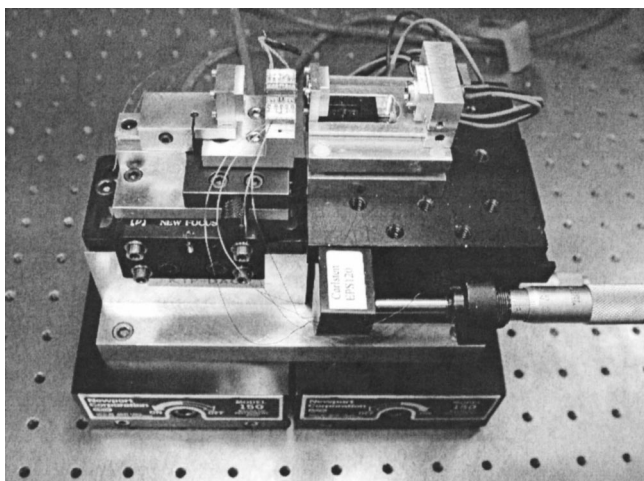


**Fig. 6** Optical setup for the alignment and testing of the external cavity diode laser.

waveguide is accomplished by using a four-axis positioner (New Focus 9071). The KTP substrate is temperature stabilized using a commercial temperature controller to monitor a thermistor and adjust the current to a thermoelectric cooler placed below the KTP substrate and electrode assembly.

The output light from the waveguide was collected by a collimating lens and was incident on a single-mode optical fiber. The output from the single-mode optical fiber was input into an Advantest Q8381A optical spectrum analyzer. The resolution of the optical spectrum analyzer is 0.1 nm. The laser diode without optical feedback has a center wavelength of 796 nm. The diode laser was coupled into waveguide number 4, which has a maximum Bragg reflectivity at 793.28 nm predicted by the numerical modeling of the super Bragg grating. The optical feedback from the Bragg grating forces the laser diode to operate at the 793.28 nm. A plot of the output power as a function of wavelength is shown in Fig. 7. The optical spectrum for the free-running diode laser has a center wavelength near 796 nm and runs multimode. The optical spectrum for the waveguide-based external-cavity diode laser (ECDL) is also shown in Fig. 7. The output of the external cavity laser is operating at 793.3 nm, which corresponds to the prediction from the numerical modeling and operates in a single mode. The sidemode suppression ratio is measured at greater than 35 dB. The output power of the laser was measured at 3 mW. Waveguides 1 to 8 were tested in a similar manner and good agreement between the predicted and measured operating wavelengths was seen.

The electrodes, as described in the previous section, were aligned over the super Bragg grating contained in waveguide number 4. Applying a voltage across the waveguide changes the index of refraction and thus changes the Bragg grating spacing. This forces a new Bragg condition causing the laser to tune. A plot of the relative frequency of the laser as a function of voltage is shown in Fig. 8. A Thor Labs piezoelectric transducer (PZT) voltage source was used to apply a voltage in 0.1-V increments across the electrodes used to tune the laser. A Burleigh Wavemeter WA-1500 was used to measure the relative frequency of the laser output.

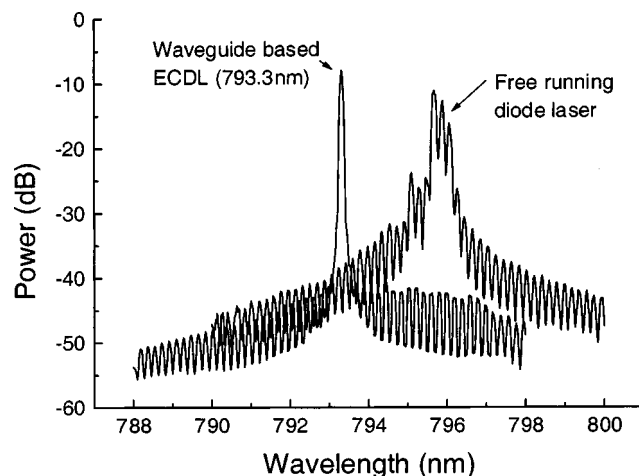


**Fig. 7** Measured spectral output of the diode laser. The free-running diode laser operates multimode near a center wavelength of 796 nm. The waveguide-based ECDL runs single mode with the optical feedback forcing the laser to operate at 793.3 nm with a sidemode suppression ratio of 35 dB. The expected operating wavelength based on the numerical modeling of the super Bragg grating is 793.28 nm.

The circles in Fig. 8 represent the measured values while the solid line is a linear fit to the data. The slope of the linear fit gives the tuning response of the laser and is  $R = 19.5 \text{ MHz/V}$ .

## 5 Conclusions

The design of a tunable ECDL based on waveguide structures and integrated optics was presented. The waveguide structures were created through ion diffusion of Rb that replaces the K in the KTP crystal. Areas of high Rb concentration increase the index of refraction by approximately 0.1%, allowing for waveguide structures and integrated optics such as Bragg gratings.

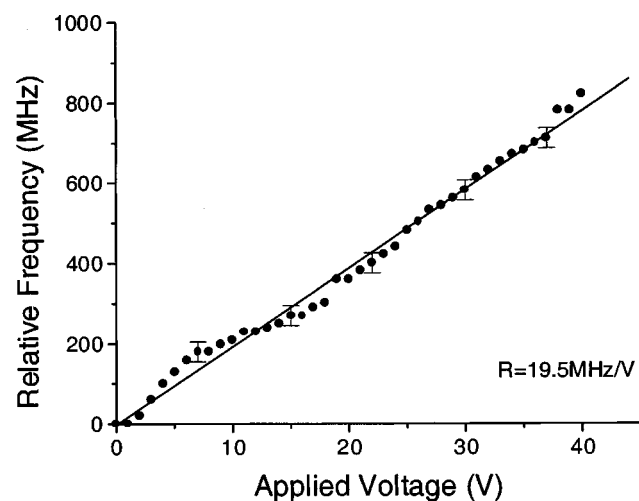


**Fig. 8** Measured electro-optic tuning of the Bragg-stabilized diode laser. The circles represent measurements, while the solid line is a linear fit to the data. A response of  $R = 19.5 \text{ MHz/V}$  was demonstrated.

A tunable laser built at 793 nm was demonstrated. This laser used the reflection from a super Bragg grating to provide optical feedback and control the operating wavelength of the laser. Tuning via the electro-optic effect was demonstrated with a measured tuning response of  $R = 19.5 \text{ MHz/V}$ .

### Acknowledgments

This work was supported by a grant from the Montana Board of Research and Commercialization and the National Science Foundation Partnership for Innovation Program (Award No. 0125429). The first author would like to thank Rand Swanson for his help in the modeling of the Bragg grating.

### References

1. USF HITRAN-PC, Ontar Corporation, North Andover, MA (1996).
2. H. I. Schiff, "Measurement of atmospheric gases," *Proc. SPIE* **1433**, ix-x (1991).
3. A. Fried, D. K. Killinger, and H. I. Schiff, "Tunable diode laser spectroscopy, lidar, and dial techniques for environmental and industrial measurements," *Proc. SPIE* **2112**, ix-x (1993).
4. C. E. Wieman and L. Hollberg, "Using diode lasers for atomic physics," *Rev. Sci. Instrum.* **62**, 1-20 (1991).
5. J. A. Reagan, T. W. Cooley, and J. A. Shaw, "Prospects for an economical, eye safe water vapor LIDAR," in *Proc. International Geoscience and Remote Sensing Symposium*, pp. 872-874, Tokyo (1993).
6. H. I. Schiff, J. Bechara, J. T. Pisano, and G. I. Mackay, "Measurements of  $\text{CH}_4$  and  $\text{C}_2\text{H}_6$  in the emissions from aluminum smelters by tunable diode laser absorption spectrometry," *Proc. SPIE* **2112**, 81-86 (1993).
7. M. de Labachellerie and G. Passadat, "Mode-hop suppression of Littrow grating tuned lasers," *Appl. Opt.* **32**, 269-274 (1993).
8. D. Wandt, M. Laschek, K. Przyklenk, A. Tunnermann, and H. Welling, "External cavity laser diode with 40 nm continuous tuning range around 825 nm," *Opt. Commun.* **130**, 81-84 (1996).
9. F. Schael, L. Hildebrandt, R. Knispel, and J. Sacher, "Robust external cavity diode lasers (ECDL) and their applications in water vapor and saturated-absorption rubidium spectroscopy," *Tech. Digest Opt. Soc. Am.* **36**, 97-98 (2000).
10. J. Lazar, O. Cip, and P. Jedlicka, "Tunable extended cavity diode laser stabilized on iodine at  $\lambda = 633 \text{ nm}$ ," *Appl. Opt.* **39**, 3085-3088 (2000).
11. M. G. Roelofs, P. A. Morris, and J. D. Bierlein, "Ion exchange of Rb, Ba, and Sr in  $\text{KTiOPO}_4$ ," *J. Appl. Phys.* **70**, 720-728 (1991).
12. L. Li and J. Burke, "Linear propagation characteristics of periodically segmented waveguides," *Opt. Lett.* **17**, 1195-1197 (1992).
13. D. K. Mynbaev and L. L. Scheuner, "Optical fibers—a deeper look," in *Fiber-Optic Communications Technology*, Prentice Hall, Upper Saddle River, NJ (2001).
14. K. S. Repasky, G. W. Switzer, and J. L. Carlsten, "Design and performance of a frequency chirped external cavity diode laser," *Rev. Sci. Instrum.* **73**, 3154-3159 (2002).
15. A. Yariv, "The modulation of optical radiation," in *Quantum Electronics*, 2nd ed., Wiley, New York (1975).

**Kevin S. Repasky** received his BSEng degree in mechanical engineering from Youngstown State University in 1988 and his MS and PhD degrees in physics from Montana State University in 1992 and 1996, respectively. He is currently working in the field of laser source development. He has recently worked on external-cavity diode lasers, mode-locked fiber lasers, cw optical parametric oscillator (OPO) lasers, and cw Raman lasers. He is also working in the field of atmospheric remote sensing.

**Jennifer D. Williams** received an AA degree in humanities from Central Oregon Community College in 1998. She is currently a junior at Montana State University working toward her BS degree in physics with minors in philosophy and mathematics. She has been characterizing KTP waveguides and electro-optically tuned diode lasers. She is currently working on laser source development at Montana State University.

**John L. Carlsten** received his BS degree in physics from the University of Minnesota in 1996 and his MS and PhD degrees in physics from Harvard University in 1974. Currently, he is a Regents Professor at Montana State University. Previously he was with at the University of Colorado from 1974 to 1979 and the Los Alamos National Laboratory from 1979 to 1984. His current research involves the study of the diode-pumped Raman laser and the application of diode lasers to fiber optics. He is also actively involved in the transfer of diode laser technology to the local optics industry in Bozeman, Montana.

**Elizabeth J. Noonan** received a BS degree in mathematics and French translation from St. Mary-of-the-Woods College in 1989, a second BS in physics in 1999 and her MS degree in physics in 2001, both from Montana State University. She has spent a year in graduate school working with the design and characterizations of KTP waveguides. Noonan joined AdvR, Inc., in Bozeman, Montana, in August 2002.

**Gregg W. Switzer** received his PhD degree in physics from Montana State University in 1998. His recent work involved developing a high-power, single-mode, narrow-linewidth pulsed laser diode transmitter at 935 nm in collaboration with the National Aeronautics and Space Administration (NASA) Goddard Space Flight Center. This laser transmitter was used to demonstrate the feasibility of a proposed minilidar system that could measure atmospheric water vapor from the surface of Mars. Dr. Switzer's research interests include semiconductor lasers, fiber optics, high-finesse Fabry-Pérot interferometers, spectroscopy, and trace gas detection using diode-based lidar systems. Dr. Switzer joined AdvR, Inc., in Bozeman, Montana, in September 1999.